

Syntheses and Reactivity of Cationic Borane–Ruthenium Complexes $[(\eta^5\text{-C}_5\text{R}_5)\text{Ru}(\text{PMe}_3)_2(\eta^1\text{-BH}_3\cdot\text{EMe}_3)][\text{BAR}^f_4]$ ($\text{R} = \text{H, Me; E} = \text{N, P;}$ $\text{BAR}^f_4 = [\text{B}\{3,5\text{-C}_6\text{H}_3(\text{CF}_3)_2\}_4]$)

Yasuro Kawano,* Masahiro Hashiva, and Mamoru Shimoi*

Department of Basic Science, Graduate School of Arts and Sciences, University of Tokyo,
 Meguro-ku, Tokyo 153-8902, Japan

Received May 18, 2006

Chloride displacement from $[(\eta^5\text{-C}_5\text{R}_5)\text{Ru}(\text{PMe}_3)_2\text{Cl}]$ by $\text{Na}[\text{BAR}^f_4]$ in the presence of $\text{BH}_3\cdot\text{EMe}_3$ afforded cationic borane σ complexes containing an unsupported B–H–Ru bridge, $[(\eta^5\text{-C}_5\text{R}_5)\text{Ru}(\text{PMe}_3)_2(\eta^1\text{-BH}_3\cdot\text{EMe}_3)][\text{BAR}^f_4]$ (**4a**: $\text{R} = \text{H, EMe}_3 = \text{PMe}_3$; **4b**: $\text{R} = \text{Me, EMe}_3 = \text{PMe}_3$; **4c**: $\text{R} = \text{H, EMe}_3 = \text{NMe}_3$; $[\text{BAR}^f_4] = [\text{B}\{3,5\text{-C}_6\text{H}_3(\text{CF}_3)_2\}_4]$). Compounds **4a–c** were fully characterized, and their structures were determined by X-ray crystallographic analysis. In these complexes, the borane ligand is coordinated to the ruthenium atom through a B–H–Ru three-center two-electron bond. They exhibit fluxional behavior due to site exchange between the BH hydrogen atoms. Complexes **4a** and **4c** are remarkably stable. However, they are hydrolyzed by a trace amount of water to produce a cationic dihydride, *trans*- $[\text{CpRuH}_2\text{-}(\text{PMe}_3)_2]^+$ (**6**, $\text{Cp} = \eta^5\text{-C}_5\text{H}_5$). The reactivity of **4a** toward various substrates was investigated.

Introduction

Activation of an inert p-block element–hydrogen σ bond by a transition metal complex has been an important subject in organometallic chemistry. In particular, CH bond activation of alkanes has been attracting much interest.¹ How do the most inert species, alkanes, interact with transition metals? This is quite a fundamental issue in coordination chemistry. It is also of importance for the effective use of petroleum resources. In many cases, alkane activation (oxidative addition/reductive elimination) is thought to proceed through an intermediate alkane σ complex.² However, owing to their extremely labile nature, investigation of alkane complexes has been performed at very low temperature or by the use of flash photolysis techniques.³ Thus, the structure and properties of alkane complexes have not been established in detail.⁴

Monoborane–Lewis base adducts, $\text{BH}_3\cdot\text{L}$ ($\text{L} =$ neutral Lewis base), are charge-neutral and isoelectronic with alkanes. Because

of this relationship, study of the coordination chemistry of borane–Lewis base adducts would be of interest in that it might have an impact not only on boron chemistry but also on basic coordination chemistry including alkane activation. During the course of our study on this subject, we have obtained several borane σ complexes, in which a BH σ bond acts as a two-electron donor.^{5–7} For example, the complexes $[\text{M}(\text{CO})_5(\eta^1\text{-BH}_3\cdot\text{L})]$ (**1**: $\text{M} = \text{Cr, W; L} = \text{NMe}_3, \text{PMe}_3, \text{PPh}_3$) and $[\text{CpMn}(\text{CO})_2(\eta^1\text{-BH}_3\cdot\text{L})]$ (**2**: $\text{L} = \text{NMe}_3, \text{PMe}_3$) were synthesized by photolyses of the respective metal carbonyl in the presence of $\text{BH}_3\cdot\text{L}$ adducts. They were isolated as crystalline solids, and their structures were determined by X-ray diffraction. These compounds are equivalent to transient alkane complexes, $[\text{M}(\text{CO})_5(\text{alkane})]$ (**A**)⁸ and $[\text{CpMn}(\text{CO})_2(\text{alkane})]$,⁹ $[\text{CpRe}(\text{CO})_2(\text{alkane})]$ (**B**),¹⁰ respectively (Chart 1). The coordinated borane adduct is so labile that compounds **1** and **2** decompose in a few days at room temperature through borane dissociation.

Theoretical calculations provided information on the nature of the borane–metal bonding in these complexes. The BH σ orbital is largely stabilized by interaction with the metal d_σ orbital. On the other hand, the high energy of the BH σ^* orbital prevents metal back-donation into this antibonding orbital. The borane–metal interaction can thus be described as a combination of the predominant borane-to-metal electron donation and very

* Corresponding authors. E-mail: ykawano@mbh.nifty.com; cshimoi@mail.ecc.u-tokyo.ac.jp.

(1) For example: (a) Shilov, A. E.; Shul'pin, G. B. *Chem. Rev.* **1997**, *97*, 2879. (b) Catalysis by Metal Complexes, VI, 21. *Activation and Catalytic Reactions of Saturated Hydrocarbons in the Presence of Metal Complexes*; Shilov, A. E., Shul'pin, G. B., Eds.; Kluwer: Dordrecht, 2000.

(2) For example: (a) Ziegler, T.; Tschinke, V.; Fan, L.; Becke, A. D. *J. Am. Chem. Soc.* **1989**, *111*, 9177. (b) Periana, R. A.; Bergmann, R. G. *J. Am. Chem. Soc.* **1986**, *108*, 7332. (c) Bullock, R. M.; Headford, C. E. L.; Hennessy, K. M.; Kegley, S. E.; Norton, J. R. *J. Am. Chem. Soc.* **1989**, *111*, 3897. (d) Gould, G. L.; Heinekey, D. M. *J. Am. Chem. Soc.* **1989**, *111*, 5502. (e) Wick, D. D.; Reynolds, K. A.; Jones, W. D. *J. Am. Chem. Soc.* **1999**, *121*, 3974. (f) Mobley, T. A.; Schade, C. Bergmann, R. G. *J. Am. Chem. Soc.* **1995**, *117*, 7822.

(3) For example: (a) Kubas, G. J. *Metal Dihydrogen and σ -Bond Complexes*; Kluwer Academic/Plenum Publishers: New York, 2001; pp 365–415. (b) Hall, C.; Perutz, R. N. *Chem. Rev.* **1996**, *96*, 3125, and references therein.

(4) Two reports have documented crystallographic evidence of significant interactions between an alkane and a metal center. In these works, however, the metal-coordinated hydrogen atoms were not located directly. (a) *n*-Heptane-double A-frame porphyrin iron(II) complex: Evans, D. R.; Drovetskaya, T.; Bau, R.; Reed, C. A.; Boyd, P. D. W. *J. Am. Chem. Soc.* **1997**, *119*, 3633. (b) Alkane-macrocyclic ligand uranium(III) complexes: Castro-Rodriguez, I.; Nakai, H.; Gantzel, P.; Zakharov, L. N.; Rheingold, A. L.; Meyer, K. J. *Am. Chem. Soc.* **2003**, *125*, 15734.

(5) Shimoi, M.; Nagai, S.; Ichikawa, M.; Kawano, Y.; Katoh, K.; Uruichi, M.; Ogino, H. *J. Am. Chem. Soc.* **1999**, *121*, 11704.

(6) Kakizawa, T.; Kawano, Y.; Shimoi, M. *Organometallics* **2001**, *20*, 3211.

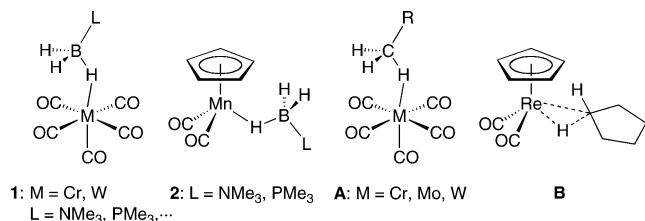
(7) Yasue, T.; Kawano, Y.; Shimoi, M. *Angew. Chem., Int. Ed.* **2003**, *42*, 1727.

(8) For example: (a) Graham, M. A.; Poliakov, M.; Turner, J. J. *J. Chem. Soc. (A)* **1971**, 2939. (b) Sun, X.-Z.; Grills, D. C.; Nikiforov, S. M.; Poliakov, M.; George, M. W. *J. Am. Chem. Soc.* **1997**, *119*, 7521. (c) Zoric, S.; Hall, M. B. *J. Phys. Chem. A* **1997**, *101*, 4646.

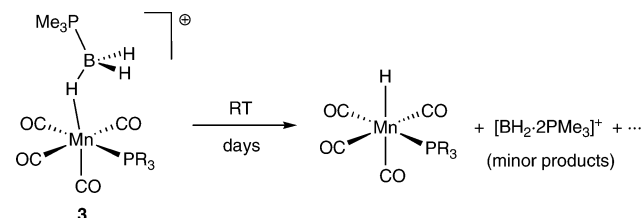
(9) (a) Klassen, J. K.; Selke, M.; Sorensen, A. A.; Yang, G. K. *J. Am. Chem. Soc.* **1990**, *112*, 1267. (b) Johnson, F. P. A.; George, M. W.; Bagratashvili, V. N.; Vereshchagina, L. N.; Poliakov, M. *Mendeleev Commun.* **1991**, 26.

(10) (a) Sun, X.-Z.; Grills, D. C.; Nikiforov, S. M.; Poliakov, M.; George, M. W. *J. Am. Chem. Soc.* **1997**, *119*, 7521. (b) Geftakis, S.; Ball, G. E. *J. Am. Chem. Soc.* **1998**, *120*, 9953. (c) Lawes, D. J.; Geftakis, S.; Ball, G. E. *J. Am. Chem. Soc.* **2005**, *127*, 4134.

Chart 1



Scheme 1



little back-donation.^{5,6} At this point, σ complexes of borane adducts are quite different from those of three-coordinate boranes, e.g., $[(\eta^5\text{-C}_5\text{H}_4\text{Me})\text{Mn}(\text{CO})_2(\text{HBX}_2)]$ ($\text{HBX}_2 = \text{HB}(1,2\text{-O}_2\text{C}_6\text{H}_4)$, pinacolborane, $\text{HB}(\text{cyclo-C}_6\text{H}_{11})_2$)¹¹ and $[\text{Cp}_2\text{Ti}(\text{HB}(1,2\text{-O}_2\text{C}_6\text{H}_4)_2)_2]$,^{12,13} in which the vacant boron p orbital accepts metal electron back-donation. Such a bonding scheme suggests a high affinity of tetracoordinate borane adducts toward positively charged metal fragments.

We have already reported a cationic manganese–borane system, $[\text{Mn}(\text{CO})_4(\text{PR}_3)(\eta^1\text{-BH}_3\cdot\text{PMe}_3)][\text{BAr}_4^-]$ (**3**, $\text{PR}_3 = \text{PMe}_2\text{-Ph}$, PET_3).⁷ Manganese boryls $[\text{Mn}(\text{CO})_4(\text{PR}_3)(\text{BH}_2\cdot\text{PMe}_3)]$ undergo protonation with a Brønsted acid with a weakly coordinating anion, $[\text{H}(\text{OEt}_2)_2][\text{BAr}_4^-]$, to produce the σ complexes. Compounds **3** decompose at room temperature in a few days to give a neutral hydride $[\text{MnH}(\text{CO})_4(\text{PR}_3)]$ and minor products including $[\text{BH}_2\cdot 2\text{PMe}_3]^+$ (Scheme 1). This indicates the occurrence of heterolytic cleavage of the metal-coordinated BH bond to form H^- and $[\text{BH}_2\cdot\text{PMe}_3]^+$. Owing to the high electrophilicity of the cationic metal center, the electron density of the borane ligand is drawn to the central metal through the bridging hydrogen atom. Such polarization induces the heterolytic cleavage of BH.¹⁴ This BH bond activation is characteristic of the cationic systems and is in sharp contrast to the neutral borane complexes, which show borane dissociation exclusively. Existence of this decomposition route hampers isolation of **3** in pure forms and thus its crystallographic analysis. Relevant heterolytic activation of H_2 and hydrosilanes on highly electrophilic $[\text{M}(\text{CO})_{5-n}(\text{PR}_3)_n]^+$ ($\text{M} = \text{Mn, Re, } n = 1, 2$) has been reported by Kubas and co-workers.^{15,16}

The aforementioned findings and insight into the M–H–B linkage imply the following inference. When the metal center is electron-rich (charge-neutral), it can interact only weakly with

Scheme 2

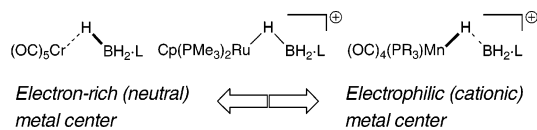
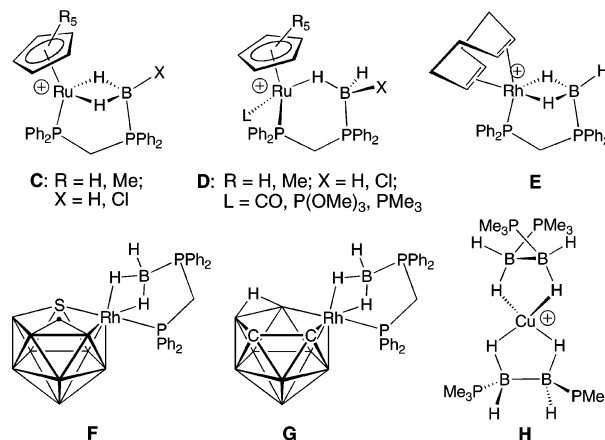


Chart 2



an electron-donating borane adduct (particularly the hydridic BH hydrogen). Thus, the M–H interaction is weak while the BH bond remains strong. Consequently, neutral borane complexes readily lose the borane ligand. On the other hand, in the cationic system **3** the metal center is so electrophilic that it effectively accepts the electron density from the borane and strongly interacts with a BH hydrogen. Accordingly, the M–H interaction is enhanced while the B–H bond is considerably weakened. If a positively charged but inherently electron-rich metal center was used, stable borane complexes containing a well-balanced B–H–M bridge could be obtained (Scheme 2). On the basis of this working hypothesis, we attempted to synthesize new borane complexes of the $[(\text{C}_5\text{R}_5)\text{Ru}(\text{PMe}_3)_2]^+$ ($\text{R} = \text{H, Me}$) metal fragment.¹⁷ As expected, we found that this 16-electron cation forms highly stable complexes with borane adducts.

While our research project was in progress, closely related compounds $[(\eta^5\text{-C}_5\text{R}_5)\text{Ru}(\eta^2\text{-BH}_2\text{X}\cdot\text{PPh}_2\text{CH}_2\text{PPh}_2)]^+$ (**C**) and $[(\eta^5\text{-C}_5\text{R}_5)\text{Ru}(\text{L})(\eta^1\text{-BH}_2\text{X}\cdot\text{PPh}_2\text{CH}_2\text{PPh}_2)]^+$ (**D**) ($\text{X} = \text{H, Cl}$) were reported by Weller and co-workers (Chart 2).^{18,19} In **C** and **D**, the phosphineborane moiety coordinates to the ruthenium atom through a monodentate or a bidentate mode and is supported by the diphosphine to form a chelate ring. Compound **C** ($\text{X} = \text{H}$) shows interesting H/D exchange on boron when it is exposed to a D_2 atmosphere. Some derivatives bearing a diphosphine-supported borane ligand have also been reported by Weller (**E**)²⁰ and Barton (**F, G**).²¹ In addition, we have reported a cationic copper complex that contains chelating diborane(4) ligands (**H**).²²

(11) Schlecht, S.; Hartwig, J. F. *J. Am. Chem. Soc.* **2000**, *122*, 9435.

(12) (a) Hartwig, J. F.; Muhoro, C. N.; He, X.; Einstein, O.; Bosque, R.; Maseras, F. *J. Am. Chem. Soc.* **1996**, *118*, 10936. (b) Muhoro, C. N.; Hartwig, J. F. *Angew. Chem., Int. Ed.* **1999**, *38*, 1510. (c) Muhoro, C. N.; He, X.; Hartwig, J. F. *J. Am. Chem. Soc.* **1999**, *121*, 5033.

(13) Lam, W. H.; Lin, Z. *Organometallics* **2000**, *19*, 2625.

(14) Crabtree, R. H. *Angew. Chem., Int. Ed. Engl.* **1993**, *32*, 789

(15) Huhmann-Vincent, J.; Scott, B. L.; Kubas, G. J. *J. Am. Chem. Soc.* **1998**, *120*, 6808.

(16) (a) Huhmann-Vincent, J.; Scott, B. L.; Kubas, G. J. *Inorg. Chim. Acta* **1999**, *294*, 240. (b) Fang, X.; Huhmann-Vincent, J.; Scott, B. L.; Kubas, G. J. *J. Organomet. Chem.* **2000**, *609*, 95. (c) Fang, X.; Scott, B. L.; John, K. D.; Kubas, G. J. *Organometallics* **2000**, *19*, 4141.

(17) Davies, S. G.; McNally, J. P.; Smallridge, A. *J. Adv. Organomet. Chem.* **1990**, *30*, 1.

(18) Merle, N.; Kocok-Köhn, G.; Mabon, M. F.; Frost, C. G.; Ruggerio, G. D.; Weller, A. S. *Dalton Trans.* **2004**, 3883.

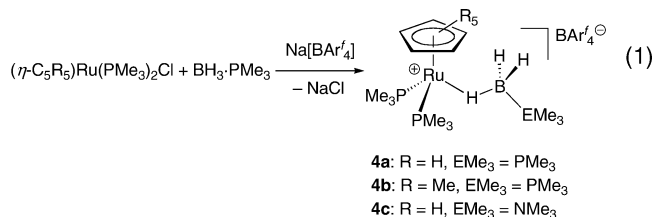
(19) Merle, N.; Frost, C. G.; Kocok-Köhn, G.; Willis, M. C.; Weller, A. S. *J. Organomet. Chem.* **2005**, *690*, 2829.

(20) Ingleson, M.; Patmore, N. J.; Ruggerio, G. D.; Frost, C. G.; Mahon, M. F.; Willis, M. C.; Weller, A. S. *Organometallics* **2001**, *20*, 4434.

(21) (a) Macías, R.; Rath, N. P.; Barton, L. *Angew. Chem., Int. Ed.* **1999**, *38*, 162. (b) Volkov, O.; Macías, R.; Rath, N. P.; Barton, L. *Inorg. Chem.* **2002**, *41*, 5837.

Results and Discussion

Synthesis and Structures of Cationic Ruthenium Borane Complexes 4a–c. Treatment of $[\text{CpRu}(\text{PMe}_3)_2\text{Cl}]$ with $\text{Na}[\text{BARf}_4]$ in the presence of $\text{BH}_3\cdot\text{PMe}_3$ in dichloromethane gave an orange solution with concurrent precipitation of NaCl . After filtration of the salt, the solution was concentrated and cooled to $-30\text{ }^\circ\text{C}$ to yield a new borane complex, $[\text{CpRu}(\text{PMe}_3)_2(\eta^1\text{-BH}_3\cdot\text{PMe}_3)][\text{BARf}_4]$ (**4a**), as yellow crystals in 73% yield. In a similar manner, the pentamethylcyclopentadienyl derivative **4b** and the $\text{BH}_3\cdot\text{NMe}_3$ analogue of **4a**, complex **4c**, were obtained in moderate yield (eq 1).



Surprisingly, **4a** and **4c** were air-stable in the solid state. These compounds also showed remarkable thermal stability in solution. They do not reveal any signs of decomposition after 1 week in dry dichloromethane-*d*₂. Compound **4b** was somewhat heat-sensitive, so that its preparation had to be carried out below $-15\text{ }^\circ\text{C}$.

Crystals suitable for X-ray diffraction study were grown by slow diffusion of hexane vapor into their 1,2-dichloroethane (**4a** and **4c**) or dichloromethane (**4b**) solutions. Figures 1–3 exhibit the structures of the cationic moieties of **4a**, **4b**, and **4c**, respectively. The key structural parameters are listed in Table 1. In crystals of **4a** and **4b**, the cation is loosely packed in a cavity made by the bulky anions. Accordingly, they have rather large thermal ellipsoids despite the data collection being performed at 153 K. As shown in the figures, the cations adopt a three-legged piano stool geometry, and the borane ligand is coordinated to the ruthenium atom through a B–H–Ru three-center two-electron bond. The hydrogen atoms attached to boron were found by the difference Fourier syntheses, and their positions were refined isotropically. The three complexes have similar structures. In **4b**, however, the borane ligand is pushed down by the methyl groups on the five-membered ring, so that it is located at the position opposite the Cp* ligand.

The Ru···B(1) interatomic distances are 2.586(5), 2.611(6), and 2.648(3) Å for **4a**, **4b**, and **4c**, respectively. These values are much longer than the ruthenium–boron bond distance of a related borylruthenium complex, $[\text{Cp}^*\text{Ru}(\text{CO})_2(\text{BH}_2\cdot\text{PMe}_3)]$ (2.243(8) Å),²³ as well as Braunschweig's compounds $[\text{CpRu}(\text{CO})_2\text{B}(\text{NMe}_2)\text{Cl}(\text{NMe}_2)]$ and $[\text{CpRu}(\text{CO})_2\text{B}(\text{Cl})\text{NSiMe}_3\text{BCl}(\text{NSiMe}_3)]$ (2.173(3) and 2.115(2) Å, respectively).²⁴ They are also substantially longer than the ruthenium–silicon separation of a silane σ complex prepared by Lemke, $[\text{CpRu}(\text{PMe}_3)_2(\text{HSiCl}_3)]^+$, 2.329(1) Å.²⁵ Therefore, it is quite reasonable to describe the borane–metal interaction in **4** as an end-on, η^1 coordination. Weller's complexes $[(\eta^5\text{-C}_5\text{R}_5)\text{Ru}(\text{L})(\eta^1\text{-BH}_3\cdot\text{dppm})]$ (R = H, Me, L = PMe₃, P(OMe)₃, see Chart 2, **D**) have similar ruthenium–boron interatomic distances (2.499–

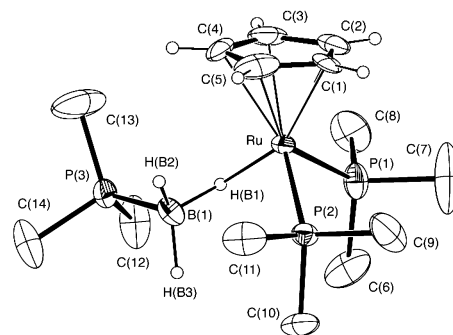


Figure 1. Structure of the cationic moiety of $[\text{CpRu}(\text{PMe}_3)_2(\eta^1\text{-BH}_3\cdot\text{PMe}_3)][\text{BARf}_4]$ (**4a**). One of the disordered Cp ligands is displayed. The thermal ellipsoids are drawn at the 30% probability level. The methyl hydrogen atoms are omitted for the sake of clarity.

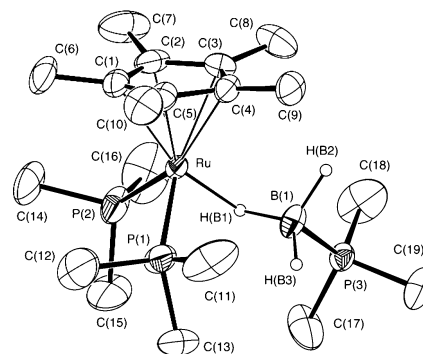


Figure 2. Structure of the cationic moiety of $[\text{Cp}^*\text{Ru}(\text{PMe}_3)_2(\eta^1\text{-BH}_3\cdot\text{PMe}_3)][\text{BARf}_4]$ (**4b**). The thermal ellipsoids are drawn at the 30% probability level. The methyl hydrogen atoms are omitted for clarity.

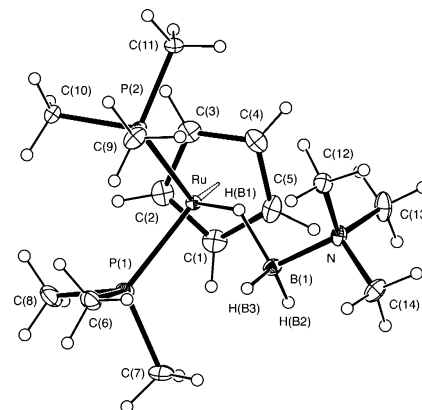


Figure 3. Structure of the cationic moiety of $[\text{CpRu}(\text{PMe}_3)_2(\eta^1\text{-BH}_3\cdot\text{NMe}_3)][\text{BARf}_4]$ (**4c**). The thermal ellipsoids are drawn at the 30% probability level.

(8)–2.5904(19) Å).¹⁸ The long Ru···B separation reflects minor back-donation into the high-lying BH σ^* orbitals.

Structural optimization of **4a** at the DFT/B3LYP level of theory reproduced the X-ray structure well, although the orientation of the borane ligand differs slightly probably because of packing effects (Figure 4). In the optimized structure, the ruthenium-coordinated BH has a bond distance of 1.274 Å, which is longer than the terminal BH bonds (1.199, 1.205 Å, Table 2). In the crystal structures, the bridging BH bond length is also comparable to or longer than the terminal BH, although the standard deviations are large (see Table 1). These phenomena

(22) Shimoi, M.; Katoh, K.; Tobita, H.; Ogino, H. *Inorg. Chem.* **1990**, 29, 814.

(23) Yasue, T.; Kawano, Y.; Shimoi, M. *Chem. Lett.* **2000**, 58.

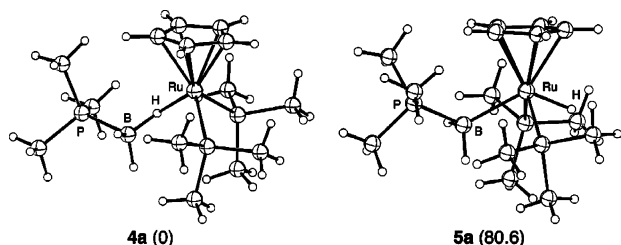
(24) (a) Braunschweig H.; Koster M.; Wang R. *Inorg. Chem.* **1999**, 38, 415. (b) Braunschweig H.; Kollann, C.; Klinkhammer K. W. *Eur. J. Inorg. Chem.* **1999**, 1523.

(25) (a) Lemke, F. R. *J. Am. Chem. Soc.* **1994**, 116, 11183. (b) Freeman S. T. N.; Lemke F. R.; Brammer, L. *Organometallics* **2002**, 21, 2030.

Table 1. Selected Interatomic Distances (Å) and Bond Angles (deg) for $[(\eta^5\text{-C}_5\text{R}_5)\text{Ru}(\text{PMe}_3)_2(\eta^1\text{-BH}_3\cdot\text{EMe}_3)][\text{BARf}_4]$ (**4a–c**)

	4a	4b	4c
CNT–Ru ^a	1.845(11)	1.885(5)	1.862(3)
Ru–P(1)	2.2729(14)	2.3069(15)	2.2996(8)
Ru–P(2)	2.3112(13)	2.2779(16)	2.2773(8)
Ru···B(1)	2.586(5)	2.611(6)	2.648(3)
Ru–H(B1)	1.92(4)	1.83(4)	1.65(3)
B(1)–H(B1)	1.28(4)	1.27(4)	1.37(3)
B(1)–H(B2)	1.26(5)	1.26(6)	1.07(3)
B(1)–H(B3)	1.30(5)	1.22(6)	1.07(3)
B(1)–E ^b	1.913(5)	1.927(6)	1.615(3)
CNT–Ru–P(1) ^a	119.7(3)	125.8(2)	122.74(12)
CNT–Ru–P(2) ^a	126.7(4)	123.6(2)	122.62(12)
CNT–Ru–H(B1) ^a	123.7(14)	128.4(17)	130.0(13)
CNT–Ru–B(1) ^a	120.5(4)	116.3(2)	122.11(13)
P(1)–Ru–H(B1)	80.8(13)	91.7(11)	94.4(11)
P(1)–Ru–B(1)	104.80(14)	82.28(16)	80.94(7)
P(2)–Ru–H(B1)	99.0(13)	79.1(12)	81.1(12)
P(2)–Ru–B(1)	81.96(12)	104.77(16)	104.05(7)
P(1)–Ru–P(2)	95.20(5)	95.30(9)	94.61(3)
Ru–H(B1)–B(1)	106(3)	113(5)	123(2)
H(B1)–B(1)–H(B2)	119(3)	115(3)	123(2)
H(B1)–B(1)–H(B3)	114(3)	122(3)	106(2)
H(B2)–B(1)–H(B3)	121(3)	113(4)	114(2)
E–B(1)–H(B1) ^b	89(2)	95.8(18)	99.8(14)
E–B(1)–H(B2) ^b	105(3)	102(3)	106.8(16)
E–B(1)–H(B3) ^b	100(2)	104(3)	103.8(18)

^a CNT = the centroid of the Cp or Cp* ligand. For **4a**, one of the disordered Cp rings is exhibited. ^b E = P(3) (**4a**, **4b**), N (**4c**).

**Figure 4.** DFT-optimized structures and relative energy (given in kJ mol^{-1}) of **4a** and **5a**.

are in agreement with the decrease of the bond order of the BH bond on coordination to the metal. Moreover, the coordinated BH bond appears to be more elongated in **4a–c** than in neutral borane complexes **1** and **2**, in which the corresponding bond distances are found to be 1.12–1.19 Å (X-ray) or around 1.25 Å (DFT).^{5,6,26,27} This is probably attributed to the pronounced polarization of the BH bond caused by the coordination to an electrophilic, positively charged ruthenium center.

DFT calculations also showed that a structural isomer, the *trans*-boryl(hydride) (**5a**), was at an energy minimum, but it was 80.6 kJ mol^{-1} higher than **4a** (Figure 4). This indicates that oxidative addition of $\text{BH}_3\cdot\text{PMe}_3$ to $[\text{RuCp}(\text{PMe}_3)_2]^+$ is unfavorable. In contrast, isoelectronic $[\text{Cp}^*\text{Ru}(\text{PMe}_3)_2\text{H}(\text{Me})]^+$ adopts a methyl(hydride) structure with a *trans* geometry. No bonding interaction is found between the methyl and hydride ligands.²⁸ The binding energy between $[\text{CpRu}(\text{PMe}_3)_2]^+$ and $\text{BH}_3\cdot\text{PMe}_3$ was calculated to be 109 kJ mol^{-1} . This value is

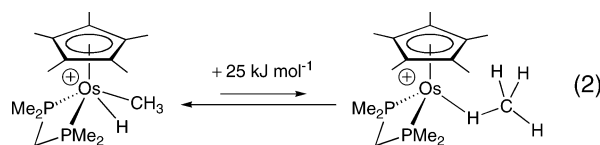
Table 2. Selected Structural Parameters in the DFT-Optimized Geometry of the Cations **4a** and **5a**

4a			
Ru···B	2.764	Ru–H	1.802
B–H(brid)	1.274	B–H(term)	1.199, 1.205
B–P	1.996	Ru–P	2.420, 2.445
Ru–H–B	127.04		
5a			
Ru–B	2.318	Ru–H(hydrido)	1.604
B–H	1.211, 1.207	B–P	2.032
Ru–P	2.421, 2.428	B–Ru–H	128.65

substantially higher than that between $[\text{Cr}(\text{CO})_5]$ and $\text{BH}_3\cdot\text{PMe}_3$ (78.6 kJ mol^{-1}).²⁹ This should be responsible for the stability of compounds **4**.

Solution Behavior of Borane Complexes 4. In the ¹¹B NMR spectra of **4**, the signal of the ruthenium-coordinated borane appeared at 5–10 ppm higher field in comparison to the corresponding free borane. Such a chemical shift change of the ¹¹B NMR signal on coordination has also been found in borane complexes that we prepared.^{5–7} In the ¹H NMR, compounds **4** display the signals of Cp, ruthenium-coordinated PMe_3 , boron-coordinated PMe_3 or NMe_3 , and the BARf_4 anion at reasonable positions. At 18 °C, **4a** exhibits only one BH resonance at –4.51 ppm as a boron-coupled broad hump with 3H intensity, indicating rapid exchange between them. This signal collapsed into the baseline at –40 °C, and at –90 °C two distinct signals appeared at –15.53 and 0.77 ppm, which are attributed to the metal-coordinated and terminal BH hydrogen atoms. The energy of activation for the fluxional process was estimated to be $38 \pm 1 \text{ kJ mol}^{-1}$ at 233 K. Likewise, the activation barrier for the BH exchange of **4b** was $36 \pm 1 \text{ kJ mol}^{-1}$ at 226 K. For the amineborane complex **4c**, the coalescence point was 10 °C, so that the BH signal was not found deceptively at ambient temperature. However, they were observed at –17.04 and 2.06 ppm at –100 °C ($\Delta G^\ddagger = 46 \pm 1 \text{ kJ mol}^{-1}$ at 283 K). Similar fluxional behaviors have been observed in other complexes of borane adducts, and the barrier for the exchange varies depending on the metal fragment and Lewis base on boron.^{5–7,27,30}

Girolami and co-workers have reported dynamic behavior of a methyl(hydride) osmium complex, $[\text{Cp}^*\text{OsH}(\text{Me})(\text{PMe}_2\text{CH}_2\text{-PMe}_2)]^+$.³¹ In the ¹H NMR spectrum, this compound shows line broadening of the methyl and hydride signals above –100 °C, indicating generation of an intermediate methane complex (through an arrested reductive elimination) and site exchange between the methane hydrogen atoms. A theoretical study showed that the methane σ complex lies ca. 25 kJ mol^{-1} above the (methyl)hydride (eq 2).^{32,33}



The fluxional behavior and optimized geometry of the osmium–methane complex resemble those of **4**. However, the relative stability of the σ complex and oxidative addition product is reversed in **4** and Girolami's compound.

(26) (a) Katoh, K.; Shimoi, M.; Ogino, H. *Inorg. Chem.* **1992**, *31*, 670. (b) Shimoi, M.; Katoh, K.; Ogino, H. *J. Chem. Soc., Chem. Commun.* **1990**, 811.

(27) Kawano, Y.; Kakizawa, T.; Yamaguchi, K.; Shimoi, M. *Chem. Lett.* **2006**, *35*, 568.

(28) Bryndza, H. E.; Fong, L. K.; Paciello, R. A.; Tam, W.; Bercaw, J. E. *J. Am. Chem. Soc.* **1987**, *109*, 1444.

(29) Kawano, Y.; Shimoi, M. Manuscript in preparation.

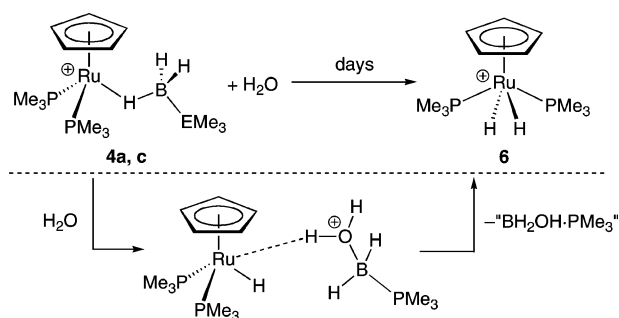
(30) Shimoi, M.; Katoh, K.; Kodama, G.; Kawano, Y.; Ogino, H. *J. Organomet. Chem.* **2002**, *659*, 102.

(31) Gross, C. L.; Girolami, G. S. *J. Am. Chem. Soc.* **1998**, *120*, 6605.

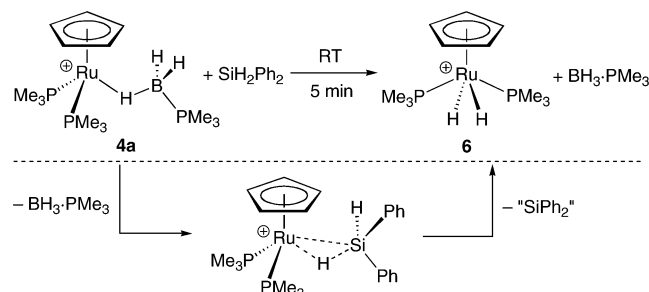
(32) Martin, R. L. *J. Am. Chem. Soc.* **1999**, *121*, 9459.

(33) Szilagyai, R. K.; Musaev, D. G.; Morokuma, K. *Organometallics* **2002**, *21*, 555.

Scheme 3



Scheme 4

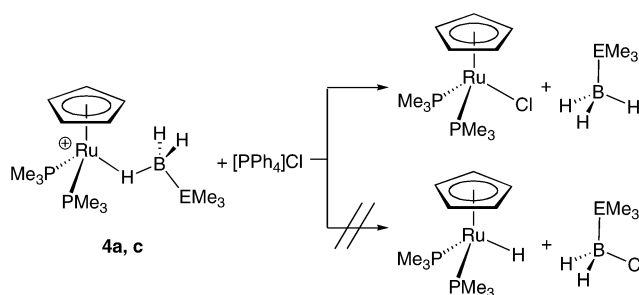


Reactivity of Ruthenium Borane Complexes. Despite the high thermal stability, compounds **4a** and **4c** are hydrolyzed by a trace amount of water to be converted into a cationic dihydride, *trans*-[CpRuH₂(PMe₃)₂]⁺ (**6**),³⁴ in several days. Hydrolysis of the deuterium-labeled derivative [CpRu(PMe₃)₂(η^1 -BD₃·PMe₃)] [BAF₄]⁻ provided the monodeuteride, [CpRuHD(PMe₃)₂]⁺. This implies heterolytic cleavage of the coordinated BH bond assisted by the attack of water (Scheme 3). Presumably, a water molecule attacks the boron atom to generate a neutral hydride [CpRuH(PMe₃)₂] and [BH₂(OH₂)·PMe₃]⁺. The electron-rich hydride is protonated by the oxonium ion to produce **6**.

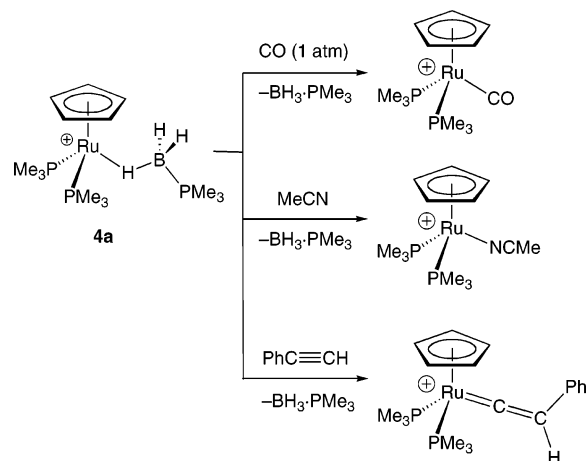
The hydrolysis of **4** is closely akin to heterolytic activation of a hydrosilane on an iron complex, [Cp*Fe(CO)(PET₃)(HSiEt₃)]⁺, reported by Brookhart. The in-situ-generated silane complex decomposes in the presence of trace water to produce [Cp*Fe(CO)(PET₃)(η^2 -H₂)]⁺. The primary step of this reaction was thought to involve heterolytic cleavage of the coordinated SiH bond; thereby [Cp*FeH(CO)(PET₃)] and [SiEt₃]⁺ were generated. The silylium ion is coordinated with water in the system, and the resulting silyloxonium ion [SiEt₃·OH₂]⁺ protonates the hydride.³⁵

Reaction of **4a** with diphenylsilane resulted in rapid formation of the dihydride **6** with dissociation of BH₃·PMe₃ (Scheme 4). When Ph₂SiD₂ was used, the dideuteride complex formed, indicating that the hydride ligands came from silane. Thus, the borane–silane exchange took place on ruthenium and was followed by double SiH activation. In fact, the SiHCl₃ complex [CpRu(PMe₃)₂(HSiCl₃)]⁺ has been isolated and structurally authenticated by Lemke.²⁵ Note that addition of Ph₂SiH₂ or Ph₃SiH to the manganese–borane complex [CpMn(CO)₂(η^1 -BH₃·NMe₃)] (**2**) provided the corresponding silane complex as a stable product.⁶

Scheme 5



Scheme 6



When **4a** or **4c** was treated with [PPh₄]Cl in dichloromethane, the chloro complex [CpRu(PMe₃)₂Cl] was produced with borane dissociation. If heterolytic cleavage of BH occurred during this reaction, BH₂Cl·PMe₃ should be formed, leaving a hydride on ruthenium. However, only simple ligand exchange was observed in this case (Scheme 5). On one hand, the triflate [PPh₄](OSO₂CF₃) did not react with **4a**, indicating that BH₃·PMe₃ coordinates to [CpRu(PMe₃)₂]⁺ more strongly than the triflate ion.

Reactions of **4a** with two-electron donors lead to simple ligand substitution (Scheme 6). Compound **4a** reacted with CO and CH₃CN to yield the corresponding carbonyl and acetonitrile complexes,³⁶ respectively. These reactions required about 12 h for completion, unlike neutral borane derivatives, **1** and **2**. Formation of the acetonitrile complex contrasts with Weller's compounds [CpRu(PR₃)(η^1 -BH₃·PPh₂CH₂PPh₂)] [PF₆]⁻ (R = Me, OMe), which were prepared by addition of BH₃·PPh₂CH₂PPh₂ and PR₃ to the acetonitrile adduct [CpRu(NCMe)₃] [PF₆]⁻.¹⁸ The reaction between **4a** and 4-(dimethylamino)pyridine (dmap) produced [CpRu(PMe₃)₂(dmap)]⁺. However, it changed into a complicated mixture after 2 h at ambient temperature. Treatment of **4a** with phenylacetylene afforded the vinylidene complex [CpRu(PMe₃)₂(=C=CHPh)]⁺.³⁷ Rearrangement of terminal alkyne π complexes to vinylidene derivatives is well known.³⁸ Also in this system, replacement of the borane ligand by the alkyne initially probably took place.

(34) (a) Lemke, F. R.; Brammer, L. *Organometallics* **1995**, *14*, 3980. (b) Brammer, L.; Klooster, W. T.; Lemke, F. R. *Organometallics* **1996**, *15*, 1721.

(35) Scharrer, E.; Chang, S.; Brookhart, M. *Organometallics* **1995**, *14*, 5686.

(36) Bruce, M. I.; Wong, F. S.; Skelton, B. W.; White, A. H. *J. Chem. Soc., Dalton Trans.* **1981**, 1398.

(37) Treichel, P. M.; Komar, D. A. *Inorg. Chim. Acta* **1980**, *42*, 277.

(38) Bustero, E.; Carbó, J. J.; Lledós, A.; Mereiter, K.; Puerta, M. C. Valerga, P. *J. Am. Chem. Soc.* **2003**, *125*, 3311.

Table 3. Crystal Data for Compounds 4a, 4b, and 4c

	4a	4b	4c
empirical formula	C ₄₆ H ₄₇ B ₂ F ₂₄ P ₃ Ru	C ₅₁ H ₅₇ B ₂ F ₂₄ P ₃ Ru	C ₄₆ H ₄₇ B ₂ F ₂₄ NP ₂ Ru
fw	1271.44	1341.57	1254.48
cryst color	yellow	yellow-orange	yellow
temperature/K	153(2)	153(2)	153(2)
wavelength	0.71073	0.71073	0.71073
cryst syst	monoclinic	monoclinic	triclinic
space group	<i>P</i> 2 ₁ / <i>n</i>	<i>P</i> 2 ₁ / <i>c</i>	<i>P</i> $\bar{1}$
<i>a</i> /Å	14.010(7)	12.668(3)	13.281(4)
<i>b</i> /Å	25.638(16)	12.786(3)	13.699(4)
<i>c</i> /Å	15.420(9)	37.507(6)	15.245(4)
α /deg	90	90	90.169(11)
β /deg	94.33(3)	100.204(7)	106.835(12)
γ /deg	90	90	95.719(11)
<i>V</i> /Å ³	5523(5)	5979(2)	2640.1(13)
<i>Z</i>	4	4	2
<i>D</i> (calcd)/Mg m ⁻³	1.529	1.490	1.578
abs coeff/mm ⁻¹	0.484	0.451	0.476
<i>F</i> (000)	2552	2712	1260
cryst size/mm	0.40 × 0.20 × 0.10	0.40 × 0.30 × 0.25	0.40 × 0.20 × 0.15
θ range/deg	3.03 to 27.49	3.19 to 27.49	2.99 to 27.48
index ranges	0 ≤ <i>h</i> ≤ 18, 0 ≤ <i>k</i> ≤ 33, −19 ≤ <i>l</i> ≤ 19	0 ≤ <i>h</i> ≤ 16, 0 ≤ <i>k</i> ≤ 16, −48 ≤ <i>l</i> ≤ 47	0 ≤ <i>h</i> ≤ 17, −17 ≤ <i>k</i> ≤ 17, −19 ≤ <i>l</i> ≤ 18
no. of indep reflns	12 591	13 612	11 949
no. of params	820	868	762
Goof on <i>F</i> ²	1.009	1.029	1.057
final <i>R</i> indices [<i>I</i> > 2σ(<i>I</i>)]	<i>R</i> 1 = 0.0486, <i>wR</i> 2 = 0.1380	<i>R</i> 1 = 0.0619, <i>wR</i> 2 = 0.1547	<i>R</i> 1 = 0.0348, <i>wR</i> 2 = 0.1019
<i>R</i> indices (all data)	<i>R</i> 1 = 0.0691, <i>wR</i> 2 = 0.1494	<i>R</i> 1 = 0.1036, <i>wR</i> 2 = 0.1795	<i>R</i> 1 = 0.0421, <i>wR</i> 2 = 1110
largest diff peak and hole/e Å ⁻³	1.041 and −0.591	0.970 and −1.128	0.506 and −0.964

Experimental Section

All manipulations were carried out under high vacuum or dry nitrogen atmosphere. Reagent-grade hexane was distilled under a nitrogen atmosphere from sodium-benzophenone ketyl immediately before use. Dichloromethane was dried over CaH₂ and distilled before use. CD₂Cl₂ was dried over 4 Å molecular sieves and vacuum-transferred into NMR tubes. BH₃·PMe₃,³⁹ [CpRu(PMe₃)₂-Cl],⁴⁰ [Cp*Ru(PMe₃)₂Cl],⁴¹ and Na[BARf₄]⁴² were prepared according to the literature. BH₃·NMe₃, PhC≡CH, AgOSO₂CF₃ (Wako Pure Chemicals), 4-(dimethylamino)pyridine (Tokyo Kasei), Ph₂-SiH₂, Ph₂SiD₂, and [PPH₄]Cl (Aldrich) were purchased and used without further purification. NMR spectra were recorded on a JEOL α-500 spectrometer. IR spectra were recorded on a Jasco FTIR-350 spectrometer.

NMR Data for [BARf₄][−]. ¹H NMR (500 MHz, CD₂Cl₂): δ 7.73 (s, 8H, ortho-H), 7.57 (s, 4H, para-H). ¹³C NMR (125 MHz, CD₂-Cl₂): δ 161.9 (q, ¹J_{BC} = 49.8 Hz, ipso-C), 135.1 (s, ortho-C), 129.1 (q, ²J_{CF} = 31.5 Hz, meta-C), 124.7 (q, ¹J_{CF} = 272.6 Hz, CF₃). ¹¹B-¹H NMR (160.35 MHz, CD₂Cl₂): δ −6.5. These data are essentially identical for compounds 4a–4c and, therefore, will not be repeated in the following paragraphs.

Synthesis of [CpRu(PMe₃)₂(η¹-BH₃·PMe₃)] [BARf₄] (4a). An H-shaped reaction tube separated with a glass filter was charged with [CpRu(PMe₃)₂Cl] (35.4 mg, 0.100 mmol), Na[BARf₄] (89.0 mg, 0.100 mmol), and BH₃·PMe₃ (12.0 mg, 0.133 mmol). Into the reaction vessel, dichloromethane (3 mL) was introduced under high vacuum at −196 °C. The resulting mixture was warmed gradually and stirred at −84 °C for 1 h and then at room temperature for 3 h. A white precipitate of NaCl was filtered, and the orange filtrate was concentrated to ca. 1 mL. The solution was diluted with hexane (1 mL) and cooled to −25 °C to provide 4a (91.3 mg, 0.072 mmol, 72%) as yellow crystals. ¹H NMR (500 MHz, CD₂Cl₂): δ 4.59 (s,

5H, C₅H₅), 1.48 (vt, ²J_{PH} = 4.6 Hz, 18H, Ru–PMe₃), 1.36 (d, ²J_{PH} = 11.5 Hz, 9H, BH₃·PMe₃), −4.51 (br, 3H, BH). The BH resonance split into two signals at −15.53 (1H, B–H–M) and 0.77 ppm (2H, terminal BH) at −90 °C. ¹¹B{¹H} NMR (160.35 MHz, CD₂Cl₂): δ −47.0 ppm (br d, ¹J_{BP} = 68 Hz). ³¹P{¹H} NMR (202.35 MHz, CD₂Cl₂): δ 5.1 (Ru–PMe₃), −3.2 (br, BH₃·PMe₃). ¹³C NMR (125 MHz, CD₂Cl₂): δ 79.1 (C₅H₅), 22.4 (vt, *J*_{PC} = 16.0 Hz, Ru–PMe₃), 11.4 (d, ¹J_{PC} = 40.3 Hz, BH₃·PMe₃). IR (Nujol mull): ν(BH) 2454.0, 2408.2 cm^{−1}. Anal. Calcd for C₄₆H₄₇B₂F₂₄P₃Ru: C, 43.45; H, 3.73. Found: C, 43.35; H, 3.85. The mass spectrum of this compound (FAB, sulfolane) gave poor data probably due to its easy fragmentation. The same was encountered in 4b and 4c.

Synthesis of [Cp*Ru(PMe₃)₂(η¹-BH₃·PMe₃)] [BARf₄] (4b). A dichloromethane solution of [Cp*Ru(PMe₃)₂Cl] (42.3 mg, 0.100 mmol), Na[BARf₄] (88.8 mg, 0.100 mmol), and BH₃·PMe₃ (11.2 mg, 0.125 mmol) was stirred under high vacuum at −84 °C for 1 h and then at −15 °C for 1 day. After filtration of NaCl, the filtrate was concentrated, diluted with hexane, and cooled to −80 °C to yield 4b (82.4 mg, 0.061 mmol, 61%) as yellow-orange crystals. ¹H NMR (500 MHz, CD₂Cl₂): δ 1.56 (s, 15H, C₅Me₅), 1.42 (vt, ²J_{PH} = 4.6 Hz, 18H, Ru–PMe₃), 1.39 (d, ²J_{PH} = 11.0 Hz, 9H, BH₃·PMe₃), −4.62 (br, 3H, BH). The last resonance was divided into two peaks at −15.62 and 0.49 ppm at −100 °C. ¹¹B{¹H} NMR (160.35 MHz, CD₂Cl₂): δ −41.8 (br, d, ¹J_{BP} = 73 Hz). ³¹P{¹H} NMR (202.35 MHz, CD₂Cl₂): δ 1.9 (Ru–PMe₃), −3.3 (q, br, BH₃·PMe₃). ¹³C NMR (125 MHz, CD₂Cl₂): δ 90.9 (C₅Me₅), 21.8 (dd, *J*_{PC} = 15.5, 14.5 Hz, Ru–PMe₃), 12.8 (d, *J*_{PC} = 40.3 Hz, BH₃·PMe₃), 11.6 (C₅Me₅). IR (Nujol mull): ν(BH) 2466.0, 2421.1 cm^{−1}. Anal. Calcd for C₅₁H₅₇B₂F₂₄P₃: C, 45.66; H, 4.28. Found: C, 44.98; H, 4.42.

Synthesis of [CpRu(PMe₃)₂(η¹-BH₃·NMe₃)] [BARf₄] (4c). This compound was prepared by a method similar to that used for 4a, using BH₃·NMe₃ instead of BH₃·PMe₃. Yellow crystalline 4c (75.6 mg, 0.06 mmol, 70%) was obtained from [CpRu(PMe₃)₂Cl] (30.4 mg, 0.086 mmol), Na[BARf₄] (77.8 mg, 0.088 mmol), and BH₃·NMe₃ (9.0 mg, 0.123 mmol). ¹H NMR (500 MHz, CD₂Cl₂): δ 4.61 (s, 5H, C₅H₅), 2.60 (s, 9H, NMe₃), 1.48 (vt, ²J_{PH} = 4.6 Hz, 18H, PMe₃). At −100 °C, the bridging and terminal BH resonances were observed at −17.04 and 2.06 ppm, respectively (2:1 intensity).

(39) Hewitt, F.; Holliday, A. K. *J. Chem. Soc.* **1953**, 530.

(40) Treichel, P. M.; Komar, D. A.; Vincenti, P. J. *Synth. React. Inorg. Met. Org. Chem.* **1984**, *14*, 383.

(41) Tilley, T. D.; Grubbs, R. H.; Bercaw, J. *Organometallics* **1984**, *3*, 274.

(42) Brookhart, M. Grant, B.; Vople, A. F., Jr. *Organometallics* **1992**, *11*, 3920.

$^{11}\text{B}\{^1\text{H}\}$ NMR (160.35 MHz, CD_2Cl_2): δ -17.5 ppm (br). ^{31}P NMR (202.35 MHz, CD_2Cl_2): δ 4.7. ^{13}C NMR (125 MHz, CD_2Cl_2): δ 79.1 (C_5H_5), 22.2 (vt, $J_{\text{PC}} = 15.9$ Hz, PMe_3), 39.9 (NMe_3). IR (Nujol mull): $\nu(\text{BH})$ 2481.5, 2437.3 cm^{-1} . Anal. Calcd for $\text{C}_{46}\text{H}_{47}\text{B}_2\text{F}_{24}\text{NP}_2\text{Ru}$: C, 44.04; H, 3.78; N, 1.12. Found: C, 44.17; H, 3.92; N, 0.93.

Hydrolysis of 4a and 4c. Dilute solutions of **4a** and **4c** in wet dichloromethane- d_2 were allowed to stand at room temperature, and ^1H and ^{11}B NMR spectra were recorded periodically. After 5 days, the resonances of $\text{trans}[\text{CpRuH}_2(\text{PMe}_3)_2]^+$ appeared with disappearance of those of **4**.

Reaction of 4a with Ph_2SiH_2 or Ph_2SiD_2 . To a dichloromethane- d_2 (0.5 mL) solution of **4a** (6.2 mg, 0.005 mmol) was added Ph_2SiH_2 (1.3 mg, 0.007 mmol) via a microsyringe at room temperature, and the ^1H NMR spectrum was recorded immediately. The spectrum indicated formation of $\text{trans}[\text{CpRuH}_2(\text{PMe}_3)_2]^+$. Likewise, Ph_2SiD_2 was added to a solution of **4a**. In the ^1H and ^2H NMR spectra of the resulting mixture, the signals of $\text{trans}[\text{CpRuD}_2(\text{PMe}_3)_2]^+$ were observed.

Reaction of 4a with $[\text{PPh}_4]\text{Cl}$. An NMR tube was charged with **4a** (5.9 mg, 0.005 mmol) and $[\text{PPh}_4]\text{Cl}$ (2.0 mg, 0.005 mmol), and CD_2Cl_2 (0.5 mL) was introduced under vacuum at -196 °C. After warming the mixture to room temperature, the ^1H and ^{11}B NMR spectra were recorded. They indicated quantitative formation of $[\text{CpRu}(\text{PMe}_3)_2\text{Cl}]$ and $\text{BH}_3\cdot\text{PMe}_3$. A similar reaction of **4c** produced $[\text{CpRu}(\text{PMe}_3)_2\text{Cl}]$ and $\text{BH}_3\cdot\text{NMe}_3$ quantitatively.

Preparation of $[\text{PPh}_4](\text{OSO}_2\text{CF}_3)$. Samples of $[\text{PPh}_4]\text{Cl}$ (250 mg, 0.67 mmol) and $\text{AgOSO}_2\text{CF}_3$ (171 mg, 0.67 mmol) were combined in CH_2Cl_2 (15 mL) and stirred at room temperature for 80 min. After filtration of precipitated AgCl , the filtrate was concentrated to ca. 1 mL. To the solution, hexane (3 mL) was added to provide $[\text{PPh}_4](\text{OSO}_2\text{CF}_3)$ (282 mg, 0.58 mol, 86%) as a white powder.

Reaction of 4a with $[\text{PPh}_4](\text{OSO}_2\text{CF}_3)$. Samples of **4a** (37 mg, 0.029 mmol) and $[\text{PPh}_4](\text{OSO}_2\text{CF}_3)$ (15 mg, 0.029 mmol) were dissolved in CD_2Cl_2 (0.5 mL). The solution was allowed to stand for 24 h, and the ^1H and ^{11}B NMR spectra were recorded. However, no reaction was observed.

Reaction of 4a with Carbon Monoxide. A CH_2Cl_2 (0.5 mL) solution of **4a** (21 mg, 0.017 mmol) was placed in an NMR tube connected to a Young's stopcock. The reaction vessel was evacuated and refilled with carbon monoxide. The contents were left at room temperature with occasional shaking. After 12 h, the yellow color of **4a** disappeared to give a very pale yellow solution. The solution was evaporated to dryness, and acetone- d_6 was introduced into the NMR tube. The ^1H NMR spectrum indicated nearly quantitative formation of $[\text{CpRu}(\text{PMe}_3)_2(\text{CO})]^+$.

Reaction of 4a with Acetonitrile. In an NMR tube, **4a** (17 mg, 0.013 mmol) was dissolved in acetonitrile (0.3 mL). The resulting solution was allowed to stand at room temperature for 12 h. Acetonitrile was removed under vacuum, and the residue was redissolved in CDCl_3 (0.5 mL). The ^1H NMR spectrum of the yellow solution indicated almost quantitative formation of $[\text{CpRu}(\text{PMe}_3)_2(\text{NCMe})]^+$.

Reaction of 4a with 4-(Dimethylamino)pyridine (dmap). Samples of **4a** (10.8 mg, 0.009 mmol) and dmap (1.4 mg, 0.012 mmol) were combined in CD_2Cl_2 at -196 °C in an NMR tube. The mixture was warmed to ambient temperature, and the reaction was monitored by ^1H NMR spectroscopy. After 10 min, 50% of **4a** was consumed, and signals of $[\text{CpRu}(\text{PMe}_3)_2(\text{dmap})]^+$ appeared along with those of free $\text{BH}_3\cdot\text{PMe}_3$. The spectrum changed into that of a complex mixture after 2 h. ^1H NMR data of $[\text{CpRu}(\text{PMe}_3)_2$ -

(dmap)] $^+$ (CD_2Cl_2) are as follows: δ 7.85, 6.30 (d, $J = 7.3$ Hz, $2\text{H} \times 2$, ring protons of dmap), 4.53 (s, 5H, C_5H_5), 2.97 (s, 6H, dmap), 1.49 (vt, $^2J_{\text{PH}} = 5.3$ Hz, 9H, PMe_3).

Reaction of 4a with Phenylacetylene. The reaction of **4a** (13.8 mg, 0.011 mmol) with phenylacetylene (1.1 mg, 0.011 mmol) was monitored by the means of NMR spectroscopy. The resulting ^1H and ^{13}C NMR spectra showed the occurrence of an instantaneous reaction to afford $[\text{CpRu}(\text{PMe}_3)_2(\text{C}=\text{CHPh})]^+$ in quantitative yield.

X-ray Crystal Structure Determination. Crystals of **4a**, **4b**, and **4c** were grown by slow diffusion of hexane into 1,2-dichloroethane (**4a**, **4c**) or dichloromethane (**4b**) solutions. Intensity data were collected on a Rigaku RAPID imaging plate diffractometer using graphite-monochromated Mo $\text{K}\alpha$ radiation ($\lambda = 0.71073$ Å). Data collection was carried out at -120 °C. Crystal data, data collection parameters, and convergence results are listed in Table 3.

Numerical absorption corrections were applied on the crystal shapes. The structures of all complexes were solved by the direct method and refined on F^2 . All non-hydrogen atoms were located and refined applying anisotropic temperature factors. Coordinates of hydrogen atoms bound to the boron atom were determined by the difference Fourier syntheses and were refined isotropically. Positions of other hydrogen atoms were idealized by using riding models. Some of the CF_3 groups in the $[\text{BArf}_4]^-$ anion were disordered around the local C_3 axis. In **4a**, the cyclopentadienyl group was also disordered over the two sites. Refinement of the positions of the carbon atoms was accomplished by the use of a rigid model with a regular pentagon. Calculations were performed using the program package SHELX 97.⁴³

DFT Calculations. The geometries of $[\text{CpRu}(\text{PMe}_3)_2(\eta^1\text{-BH}_3\cdot\text{PMe}_3)]^+$ (**4a**), $\text{trans}[\text{CpRu}(\text{H})(\text{PMe}_3)_2(\text{BH}_3\cdot\text{PMe}_3)]^+$ (**5a**), $[\text{CpRu}(\text{PMe}_3)_2]^+$, and $\text{BH}_3\cdot\text{PMe}_3$ were optimized at the B3LYP level of theory, a density functional theory (DFT) type of calculation based on hybrid functionals. A basis set with an approximation of effective core potentials, LanL2DZ, was employed for all the atoms. Vibration analyses were then performed to characterize the stationary points. Calculations were performed with the Gaussian 98W package of programs.⁴⁴

Acknowledgment. This work was financially supported by a Grant-in-Aid for Scientific Research (No. 15350193) from the Japanese Ministry of Education, Science, Sports, and Culture.

Supporting Information Available: Crystallographic information files (CIF) for **4a**, **4b**, and **4c**. This material is available free of charge via the Internet at <http://pubs.acs.org>.

OM0604324

(43) (a) Sheldrick, G. M. *SHELXS-97*; University of Göttingen, 1997. (b) Sheldrick, G. M. *SHELXL-97*; University of Göttingen, 1997.

(44) Frisch, M. J.; Trucks, G. W.; Schlegel, H. B.; Scuseria, G. E.; Robb, M. A.; Cheeseman, J. R.; Zakrzewski, V. G.; Montgomery, J. A., Jr.; Stratmann, R. E.; Burant, J. C.; Dapprich, S.; Millam, J. M.; Daniels, A. D.; Kudin, K. N.; Strain, M. C.; Farkas, O.; Tomasi, J.; Barone, V.; Cossi, M.; Cammi, R.; Mennucci, B.; Pomelli, C.; Adamo, C.; Clifford, S.; Ochterski, J.; Petersson, G. A.; Ayala, P. Y.; Cui, Q.; Morokuma, K.; Malick, D. K.; Rabuck, A. D.; Raghavachari, K.; Foresman, J. B.; Cioslowski, J.; Ortiz, J. V.; Stefanov, B. B.; Liu, G.; Liashenko, A.; Piskorz, P.; Komaromi, I.; Gomperts, R.; Martin, R. L.; Fox, D. J.; Keith, T.; Al-Laham, M. A.; Peng, C. Y.; Nanayakkara, A.; Gonzalez, C.; Challacombe, M.; Gill, P. M. W.; Johnson, B. G.; Chen, W.; Wong, M. W.; Andres, J. L.; Head-Gordon, M.; Replogle, E. S.; Pople, J. A. *Gaussian 98*, revision A.11; Gaussian, Inc.: Pittsburgh, PA, 1998.